

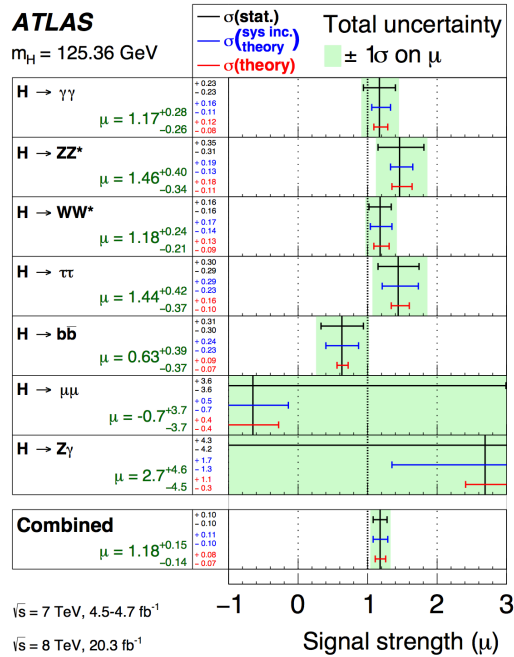


Pixel Detector For ATLAS Phase-2 Upgrade: Tracking In Very Forward Rapidity Region

Sasha Pranko
(LBNL)

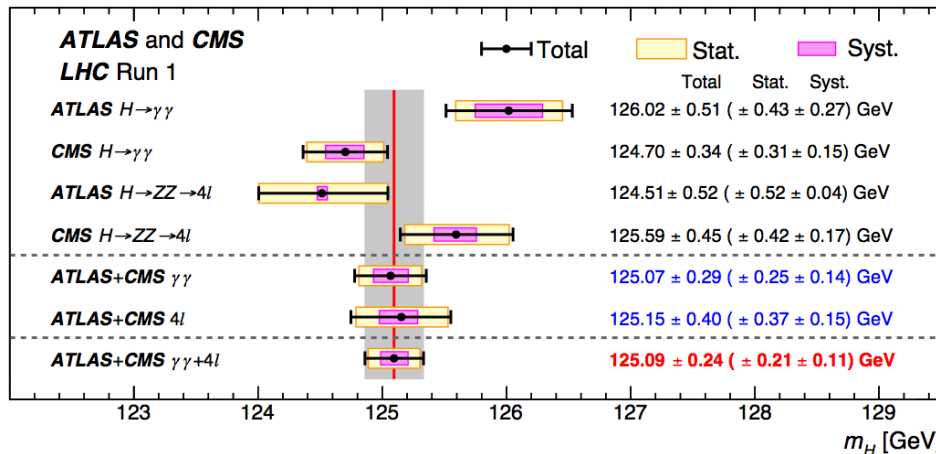
Higgs Boson Discovery: Triumph Of LHC Run-1 Program

Main Run-1 results: discovery of Higgs boson; no signs of New Physics



ATLAS SUSY Searches* - 95% CL Lower Limits
 Status: Feb 2015

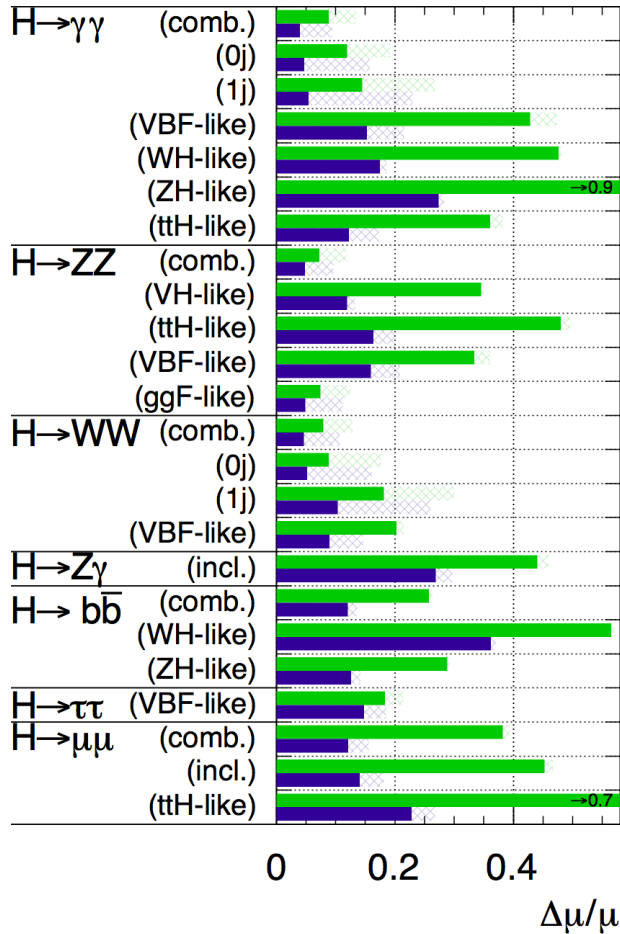
Model	$\epsilon, \mu, \tau, \gamma$	Jets	E_{T}^{miss}	[$\mathcal{L} d(\text{fb}^{-1})$]	Mass limit	Reference	
Inclusive Searches	MSUGRA/CMSSM	0 2-6 jets	Yes	20.3	$m_0 = 250 \text{ GeV}$	1405.7875	
$\tilde{g}\tilde{g} \rightarrow \tilde{g}\tilde{g}$	0 2-6 jets	Yes	20.3		850 GeV	1405.7875	
$\tilde{g}\tilde{g} \rightarrow \tilde{g}\tilde{g}$ (compressed)	1 γ 0-1 jet	Yes	20.3		250 GeV	1411.1559	
$\tilde{g}\tilde{g} \rightarrow \tilde{g}\tilde{g}$	0 2-6 jets	Yes	20.3		1.33 TeV	1405.7875	
$\tilde{g}\tilde{g} \rightarrow \tilde{g}\tilde{g} + \tilde{g}\tilde{g}$	1 e, μ 3-6 jets	Yes	20.3		1.2 TeV	1501.03555	
$\tilde{g}\tilde{g} \rightarrow \tilde{g}\tilde{g} + \tilde{g}\tilde{g}$	2 e, μ 0-3 jets	Yes	20.3		1.32 TeV	1501.03555	
GMSB (NLSP)	1-2 $\tau + 0-1 \tau$	Yes	20.3		1.6 TeV	1407.9603	
GGM (bino NLSP)	2 γ	Yes	20.3		1.28 TeV	ATLAS-CONF-2014-001	
GGM (wino NLSP)	1 $e, \mu + \gamma$	Yes	4.8		819 GeV	ATLAS-CONF-2012-144	
GGM (higgsino-bino NLSP)	7	Yes	4.8		900 GeV	121.1167	
GGM (higgsino NLSP)	2 e, μ (Z)	0-3 jets	Yes	5.8	890 GeV	ATLAS-CONF-2012-152	
Gravitino LSP	0 mono-jet	Yes	20.3		865 GeV	1502.01518	
3γ gen. sparticles & med. GMSB	$\tilde{g} \rightarrow \tilde{g}\tilde{g}$	0 3-10 jets	Yes	20.1		1.25 TeV	
$\tilde{g} \rightarrow \tilde{g}\tilde{g}$	0 7-10 jets	Yes	20.3		1.1 TeV	1407.9600	
$\tilde{g} \rightarrow \tilde{g}\tilde{g}$	0-1 e, μ 3 b	Yes	20.1		1.34 TeV	1407.9600	
$\tilde{g} \rightarrow \tilde{g}\tilde{g}$	0-1 e, μ 3 b	Yes	20.1		1.3 TeV	1407.9600	
3γ gen. sparticles direct production	$\tilde{g}_1 \tilde{g}_1 \rightarrow \tilde{g}_1 \tilde{g}_1$	0 2 b	Yes	20.1		100-620 GeV	
$\tilde{g}_1 \tilde{g}_1 \rightarrow \tilde{g}_1 \tilde{g}_1$	2 e, μ (SS)	0-3 b	Yes	20.3		275-440 GeV	
$\tilde{g}_1 \tilde{g}_1 \rightarrow \tilde{g}_1 \tilde{g}_1$	1-2 e, μ 1-2 b	Yes	4.7		110-167 GeV	220-460 GeV	
$\tilde{g}_1 \tilde{g}_1 \rightarrow \tilde{g}_1 \tilde{g}_1$ or $\tilde{g}_1 \tilde{g}_1$	2 e, μ 0-2 jets	Yes	20.3		90-191 GeV	215-530 GeV	
$\tilde{g}_1 \tilde{g}_1 \rightarrow \tilde{g}_1 \tilde{g}_1$	0 mono-jet+tag	Yes	20			210-640 GeV	
$\tilde{g}_1 \tilde{g}_1 \rightarrow \tilde{g}_1 \tilde{g}_1$	0	Yes	20.3			90-240 GeV	
$\tilde{g}_1 \tilde{g}_1 \rightarrow \tilde{g}_1 \tilde{g}_1$	2 e, μ (Z)	1 b	Yes	20.3		150-580 GeV	
$\tilde{g}_1 \tilde{g}_1 \rightarrow \tilde{g}_1 \tilde{g}_1$	3 e, μ (Z)	1 b	Yes	20.3		290-600 GeV	
EW direct	$\tilde{g}_1 \tilde{g}_1 \rightarrow \tilde{g}_1 \tilde{g}_1$	2 e, μ 0	Yes	20.3		90-325 GeV	
$\tilde{g}_1 \tilde{g}_1 \rightarrow \tilde{g}_1 \tilde{g}_1$	2 e, μ 0	Yes	20.3		140-465 GeV	1403.5294	
$\tilde{g}_1 \tilde{g}_1 \rightarrow \tilde{g}_1 \tilde{g}_1$	2 τ	Yes	20.3		100-350 GeV	1407.9550	
$\tilde{g}_1 \tilde{g}_1 \rightarrow \tilde{g}_1 \tilde{g}_1$	3 e, μ 0	Yes	20.3		700 GeV	1402.7029	
$\tilde{g}_1 \tilde{g}_1 \rightarrow \tilde{g}_1 \tilde{g}_1$	2 e, μ 0-2 jets	Yes	20.3		420 GeV	1403.5294, 1402.7029	
$\tilde{g}_1 \tilde{g}_1 \rightarrow \tilde{g}_1 \tilde{g}_1$	2 e, μ, τ	0-2 b	Yes	20.3		250 GeV	1501.07110
$\tilde{g}_1 \tilde{g}_1 \rightarrow \tilde{g}_1 \tilde{g}_1$	4 e, μ 0	Yes	20.3		820 GeV	1405.5086	
Long-lived particles	Direct $\tilde{g}_1 \tilde{g}_1$ prod., long-lived \tilde{g}_1	Disapp. trk	1 jet	Yes	20.3	270 GeV	1310.3675
Stable, stopped \tilde{g} R-hadron	0 1-5 jets	Yes	27.9			832 GeV	1310.6584
Stable \tilde{g} R-hadron	trk	-	18.1			1.27 TeV	1411.6795
GMSB, stable \tilde{g} , long-lived \tilde{g}_1	1-2 μ	-	19.1			837 GeV	1411.6795
GMSB, $\tilde{g}_1 \rightarrow \gamma G$, long-lived \tilde{g}_1	2 γ	Yes	20.3			435 GeV	1409.5542
$\tilde{g}\tilde{g}, \tilde{g}_1 \rightarrow \tilde{g}\tilde{g}$ (RPV)	1 μ , displ. vtx	-	20.3			1.0 TeV	ATLAS-CONF-2013-092
RPV	LFV $pp \rightarrow \tilde{g}_1 + X, \tilde{g}_1 \rightarrow e + \mu$	2 e, μ	-	4.6		1.61 TeV	1212.1272
LFV $pp \rightarrow \tilde{g}_1 + X, \tilde{g}_1 \rightarrow e + \mu + \tau$	1 $e, \mu + \tau$	-	4.6			1.1 TeV	1212.1272
Bilinear RPV CMSSM	2 e, μ (SS)	0-3 b	Yes	20.3		750 GeV	1405.5086
$\tilde{g}_1 \tilde{g}_1 \rightarrow \tilde{g}_1 \tilde{g}_1$	4 e, μ	-	Yes	20.3		450 GeV	1405.5086
$\tilde{g}_1 \tilde{g}_1 \rightarrow \tilde{g}_1 \tilde{g}_1$	3 $e, \mu + \tau$	-	Yes	20.3		916 GeV	1405.5086
$\tilde{g}_1 \tilde{g}_1 \rightarrow \tilde{g}_1 \tilde{g}_1$	0 6-7 jets	-	Yes	20.3		850 GeV	ATLAS-CONF-2013-091
$\tilde{g}_1 \rightarrow \tilde{g}_1, \tilde{g}_1 \rightarrow \tilde{g}_1$	2 e, μ (SS)	0-3 b	Yes	20.3		490 GeV	1404.250
Other	Scalar charm, $\tilde{c} \rightarrow c\tilde{c}$	2 c	Yes	20.3		490 GeV	1501.01325



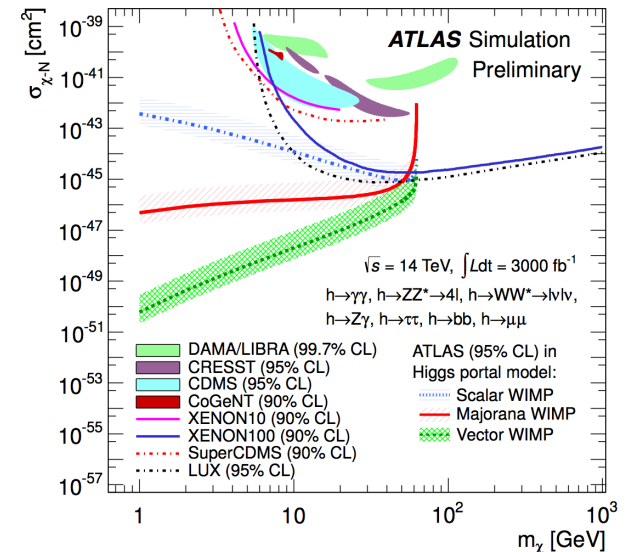
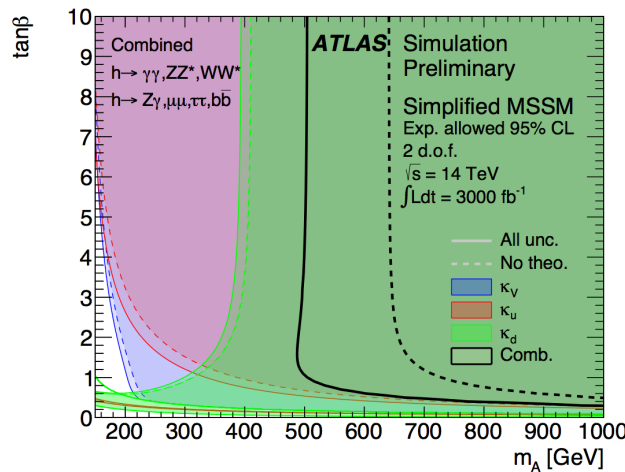
Physics Program For High Luminosity LHC

ATLAS Simulation Preliminary

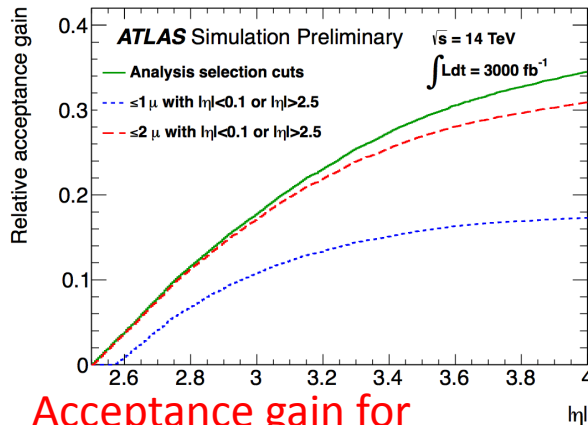
$\sqrt{s} = 14 \text{ TeV}$; $\int L dt = 300 \text{ fb}^{-1}$; $\int L dt = 3000 \text{ fb}^{-1}$



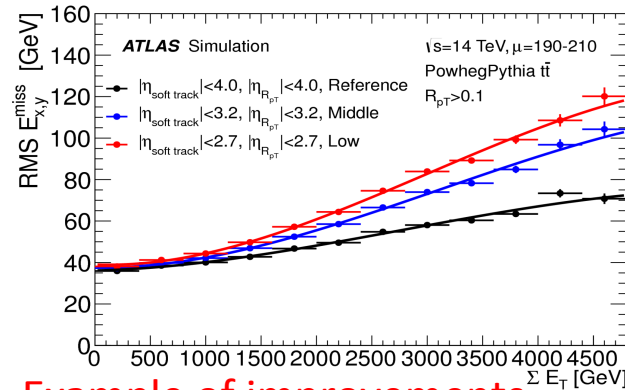
- Precision measurements of Higgs boson production and decay rates
- Observation of rare Higgs boson decays
- Search for HH production
- Search for new physics



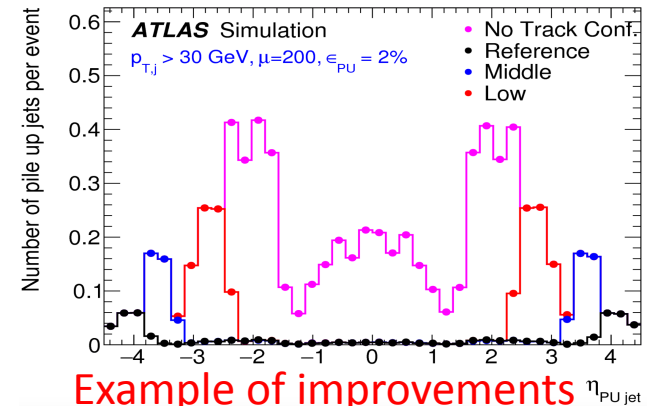
Tracking Is Crucial For Success Of HL-LHC Program



Acceptance gain for $H \rightarrow ZZ^* \rightarrow 4\mu$ decays



Example of improvements in MET resolution



Example of improvements in pile-up jet rejection

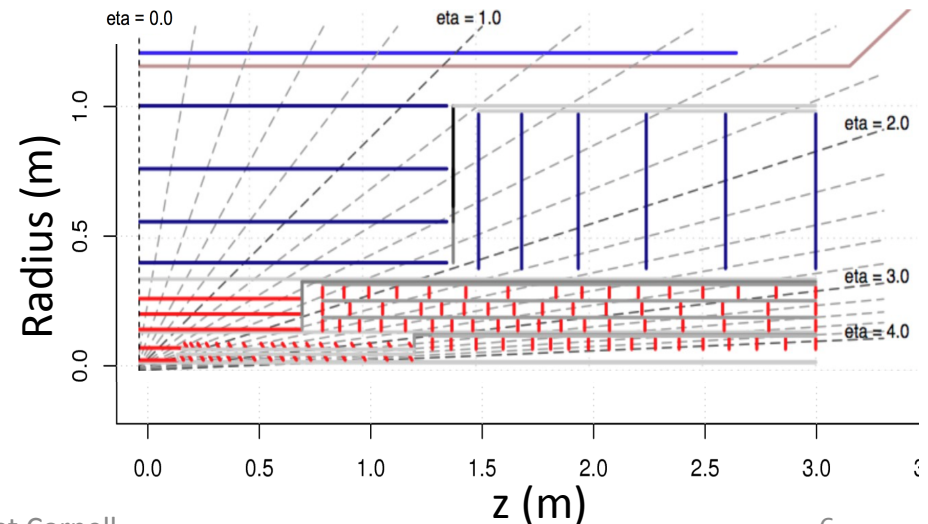
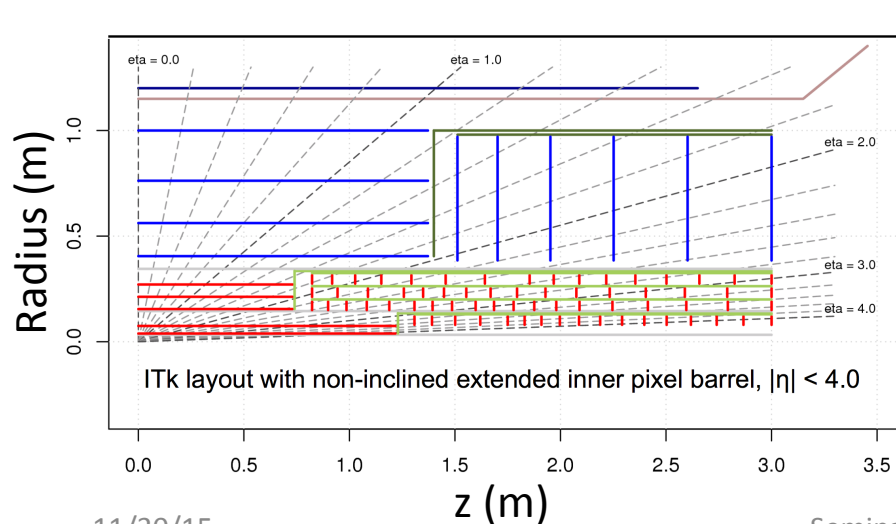
- ATLAS tracking detector during HL-LHC run will have to provide efficient and precise track reconstruction in a very challenging environment with ~ 200 pile-up interactions per bunch crossing
- New detector must cope with high radiation field (up to 7.7 MGy and $1.4 \times 10^{16} n_{eq} \text{ cm}^{-2}$)
- **All silicon tracking detector: pixel detector + strip detector**
- Extension of the tracking coverage into the very forward region (up to $|\eta| < 4$) will significantly enhance the potential of the HL-LHC physics program

Extensive R&D Program Is Well Underway

- Technical Design Report (TDR) for Strip detector is due in 2016
 - TDR for Pixel detector is due in Q4 of 2017
 - Pixel sensors (planar, 3D, CMOS,...)
 - New FE chip (RD53)
 - Module design, module electronics
 - Services
 - Local supports
 - Off-detector electronics
 - Global mechanics
 - Layout optimization
 - Software development
- } This seminar

Two Concepts Of Pixel Detector For Phase-2 Upgrade

- Tracking in the forward region ($|\eta| > 2.7$) will rely solely on Pixel detector
- Two concepts of the Pixel detector are under study
 - Concept-1 (“Extended”) utilizes long clusters from extended inner barrel layers
 - Concept-2 (“Inclined”) utilizes inclined modules in two inner barrel layers
- Two layouts under study have the same Pixel end-cap
- Both layouts are optimized to have at least 9 space points for all η
- Choose final layout based on the comparison of performance (March 2016)
- Further optimize the chosen layout to achieve most optimal performance

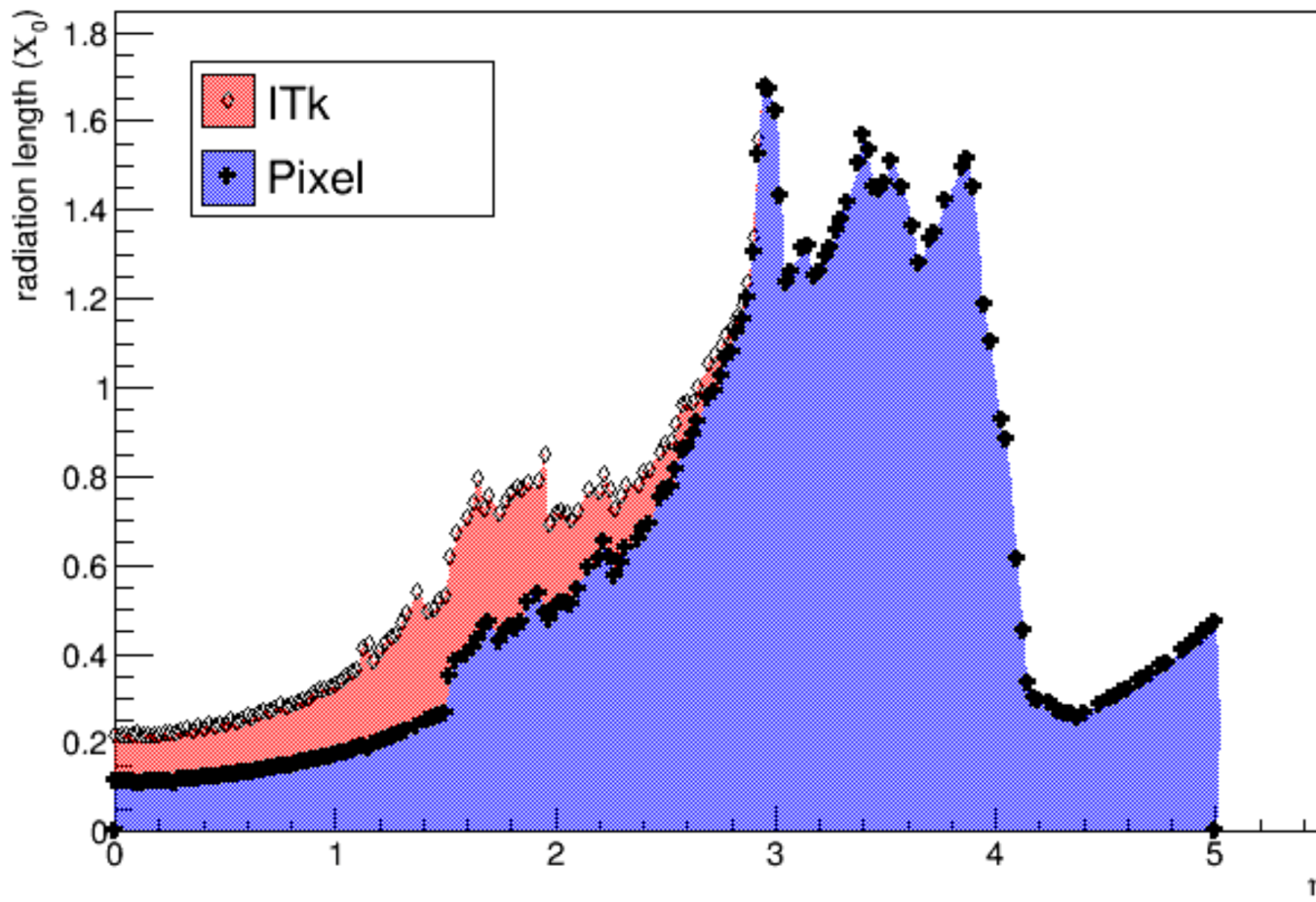


Pixel Detector For Phase-2 Upgrade

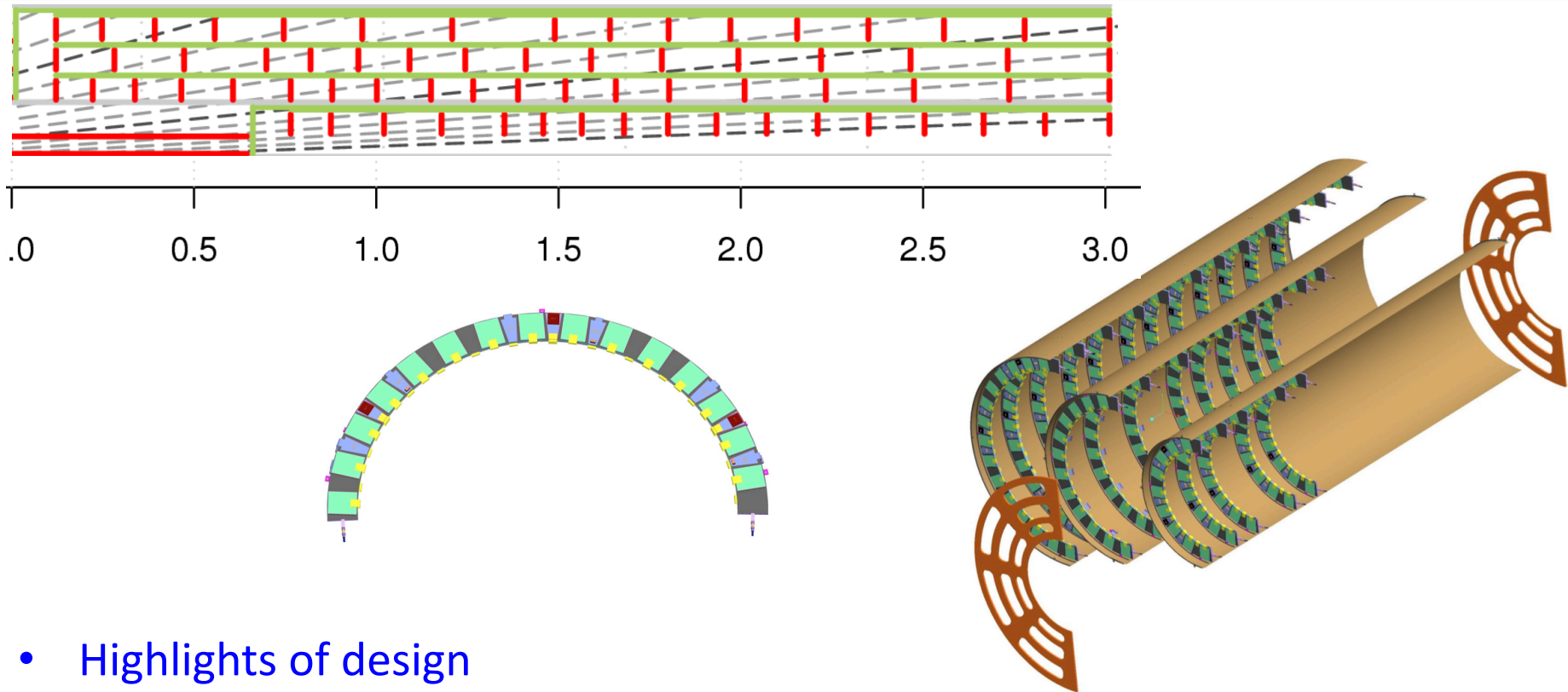
- **Sensors**
 - Planar sensors n-in-p (for now, R&D is ongoing)
 - Barrel Layer-0,1 and inner end-cap ring: $50\mu\text{m} \times 50\mu\text{m} \times 100\mu\text{m}$
 - Also consider option of $25\mu\text{m} \times 100\mu\text{m} \times 100\mu\text{m}$
 - Barrel Layer-2,3,4 & end-cap: $50\mu\text{m} \times 50\mu\text{m} \times 150\mu\text{m}$
 - Aim at operating with 600e threshold(s)
 - Electronics noise hit occupancy: 10^{-6}
- **Modules: “quad” modules everywhere (except for Layer-0, “double”)**
 - About 10,000 modules
- **Barrel: 5 layers**
 - $R=3.9, 6.5, 16, 20, 30$ cm
 - room for 6th layer, study of potential benefits are underway
- **End-cap: 4 layers of rings, number of rings vary depending in η and R**
 - $R=15-19, 21-25, 27.5-31.5, 33.5-37.5$ cm
- **Total surface is ~ 14 m²**
 - depends on layout, roughly 50/50 between barrel and end-cap
 - approximate cost is 38.5MCHF

Amount Of Material For Phase-2 ITK Detector

- Preliminary estimates for the “Extended” layout
 - This will change with more refined knowledge of services and after layout is finalized



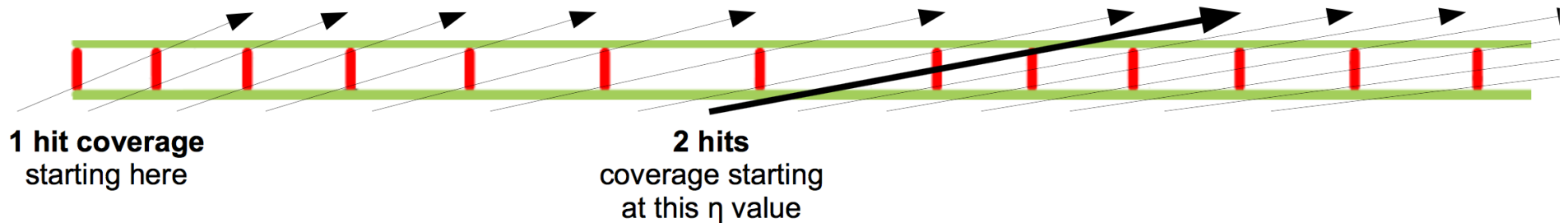
End-cap Pixel Detector



- Highlights of design

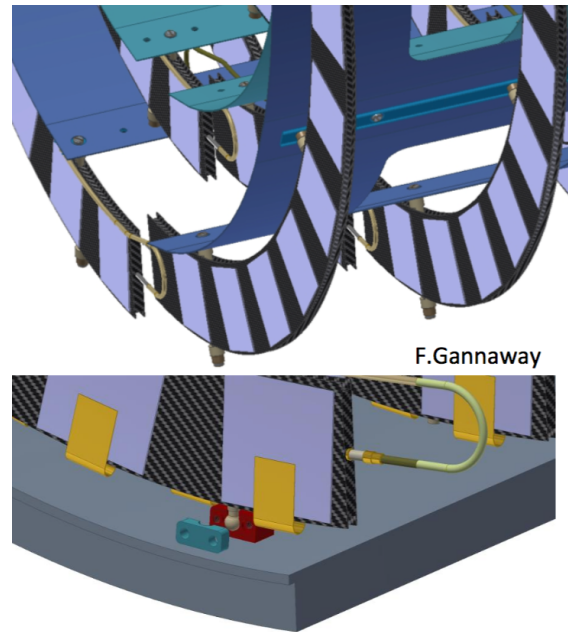
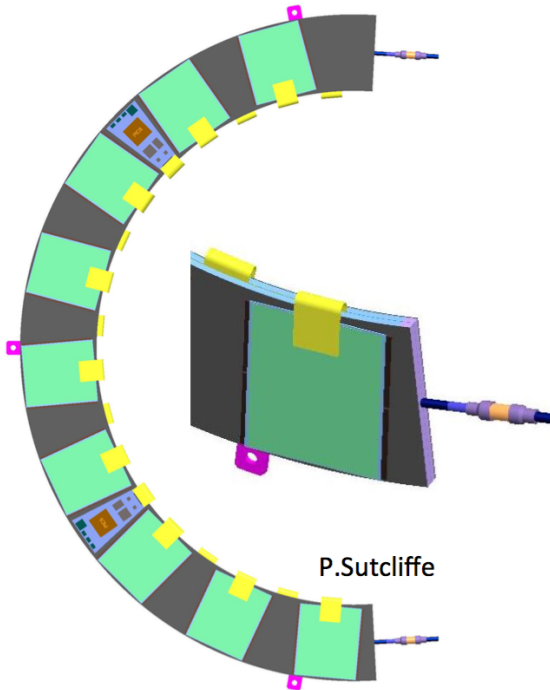
- Highly flexible design: individual rings can be placed where they are needed
- Services can be routed in between rings: greatly simplifies the build
- Use 4-chip “quad” modules: common development with barrel staves
- Highly modular design: same elements everywhere, just scale is different
- Intergration into ITK can be “monolithic” (in one piece) or “modular” (in sections)

Ring Position Optimization For End-Cap



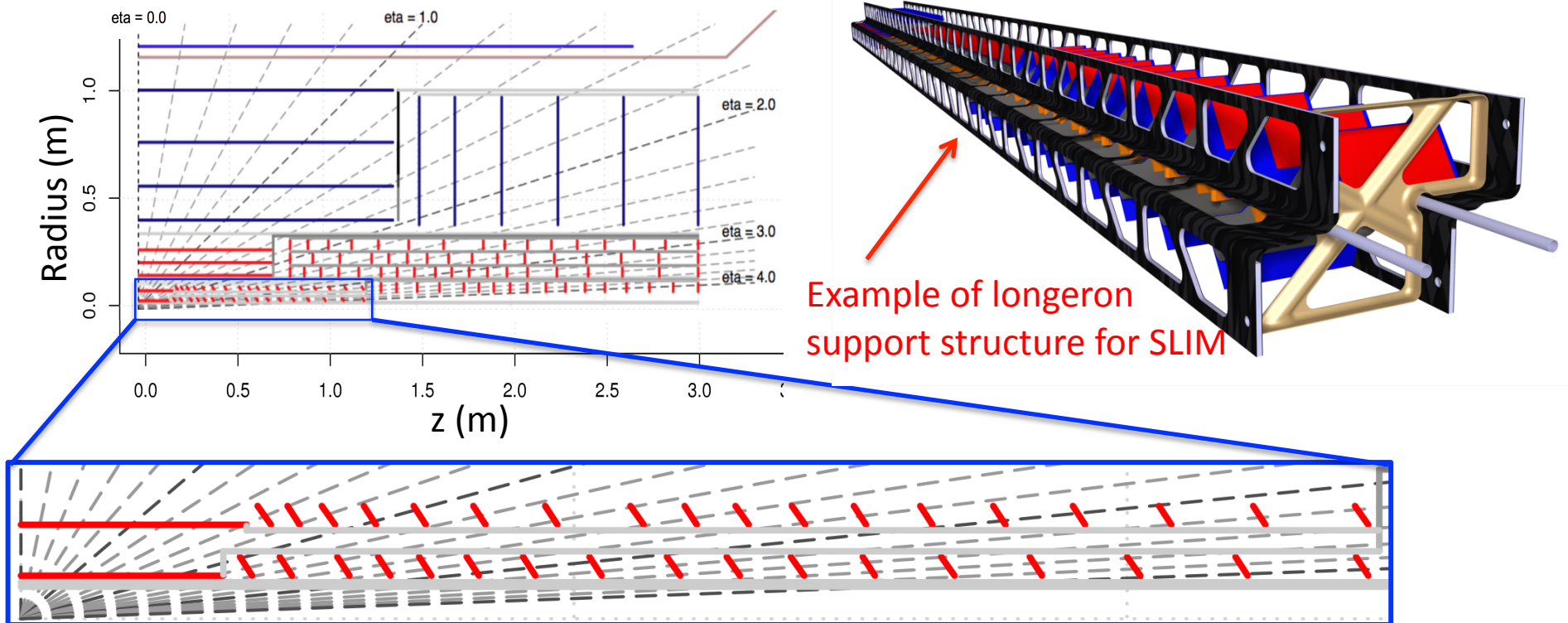
- For a given η range, each ring layer contributes a given number of hits
 - Allowing for some overlap between consecutive modules
 - Respecting a minimum distance of 8 cm between rings
- A similar principle is used for positioning the inclined barrel sensors

Ring Design For End-Cap



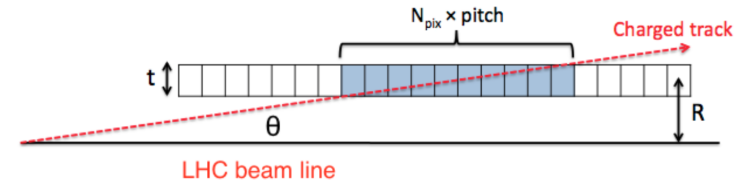
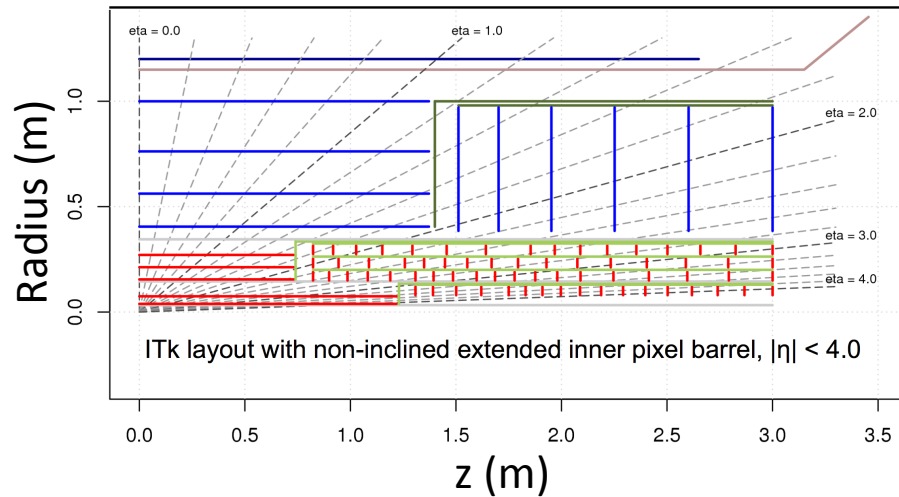
- Mechanical design is quite mature
 - Carbon fibre/foam sandwich
 - Embedded bus tape and cooling pipe
 - “Eos” card on surface for power and DCS
 - Currently assuming no GBTx–twinax routed directly from modules
- Each ring layer is attached to a support cylinder at the outer edge

“Inclined” Layout For Pixel Barrel Detector

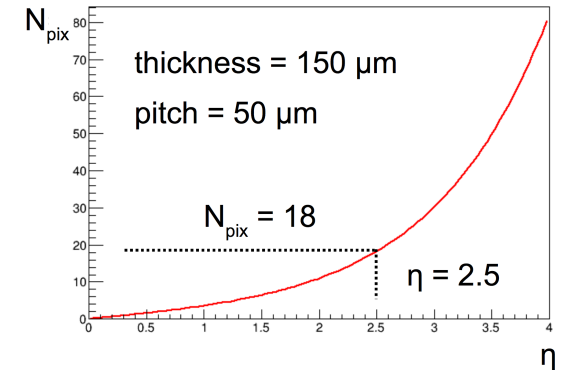


- Modules inclined at 34° with respect to vertical line
- Helps to reduce amount of material traversed by a track
 - Reduces effect of multiple scattering and silicon area
- Provides (≥ 1 for given η) hits very close to interaction point
- Two technologies: “Alpine” and SLIM

“Extended” Layout For Pixel Barrel Detector

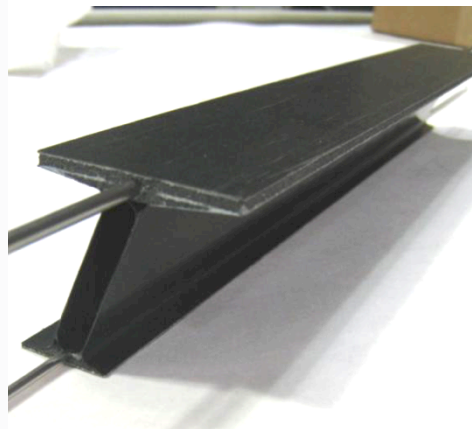
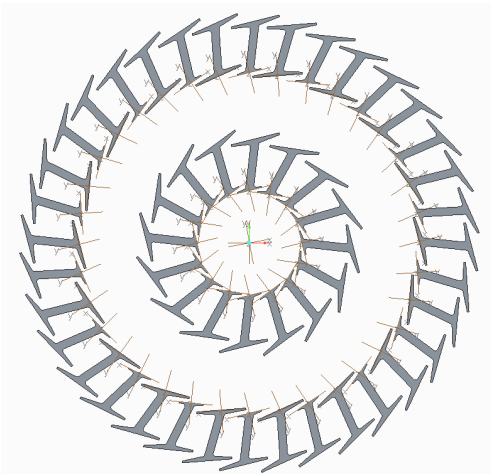


$$\tan \theta = \frac{t}{N_{pix} \times p}$$



I-beams: low-mass carbon composite support structure

- Long clusters = “tracklets”, providing initial precise estimates of θ and z_0
 - Seed pattern recognition
 - Potential to reduce fake rate
 - Potential to reduce CPU time
- Simple and easy to build design

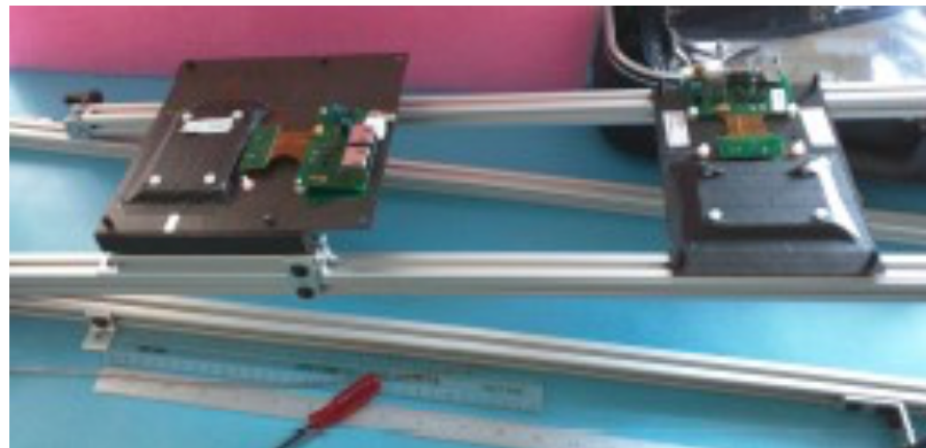
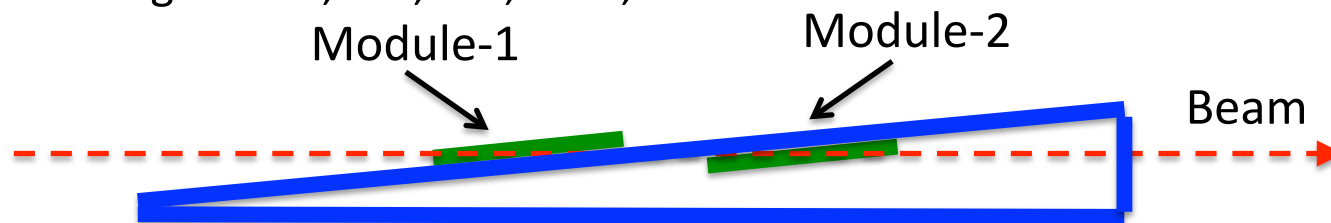


R&D Program For “Extended” Pixel Barrel Detector

- Institutions involved: **LBNL**, U. Louisville, U. Wisconsin
- Test beam to study clusters at very small incidence angles (this talk)
- Comparison of simulation with test beam results
- Development of pattern recognition based on cluster size (this talk)
- Tests of pattern recognition based on cluster size with simulation (this talk)
- Optimization of the layout
- Study of tracking performance and benefits to physics program with the optimized layout
- Test beam studies of the proto-type detector at very small incidence angles

SLAC ESA Test Beam

- Four un-irradiated Insertable B-Layer (IBL) modules
 - Two double-chip planar modules; two single-chip 3D modules
 - Most modules have FEI4B chips (one module with FEI4A chip)
 - Planar sensors: $50\mu\text{m} \times 250\mu\text{m} \times 200\mu\text{m}$
 - 3D sensors: $50\mu\text{m} \times 250\mu\text{m} \times 230\mu\text{m}$
 - Modules tuned to 10 ToT at 16K electrons
- Beam: 10 GeV electrons, a few particles per bunch at 5 Hz
 - Studies with beam in “short” ($50\mu\text{m}$) and “long” ($250\mu\text{m}$) directions
 - 5 incidence angles: $\sim 2^\circ$, $\sim 4^\circ$, $\sim 6^\circ$, $\sim 10^\circ$, $\sim 15^\circ$



CERN SPS Test Beam

- Single-chip 3D module with FEI4A chip
 - 5 incidence angles: $\sim 2^\circ$, $\sim 4^\circ$, $\sim 6^\circ$, $\sim 10^\circ$, $\sim 15^\circ$
- Beam: charged pions (π^+) with 180 GeV
- Tracks measured with FEI4 telescope with $14\mu\text{m}$ and $8.5\mu\text{m}$ resolution in X and Y

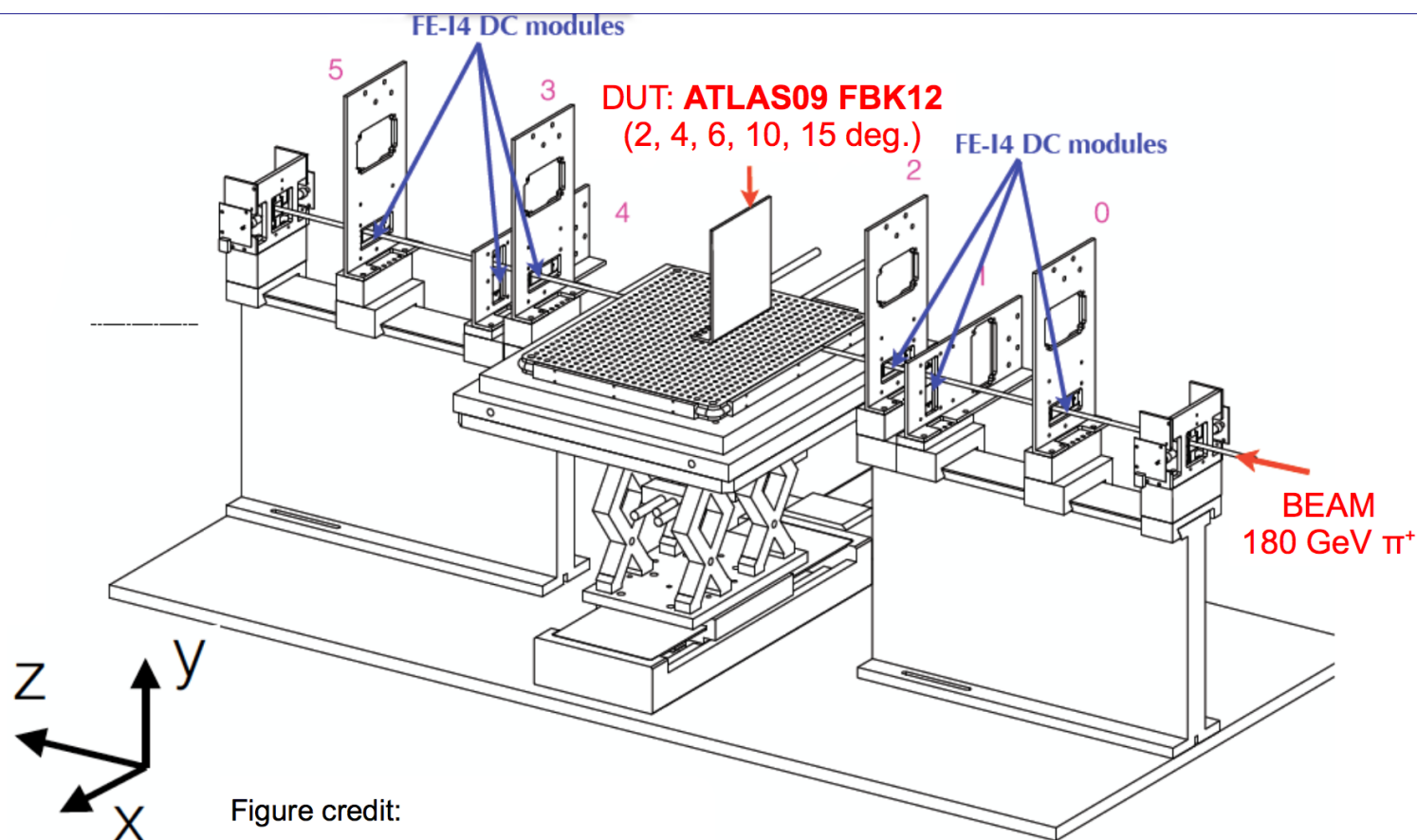
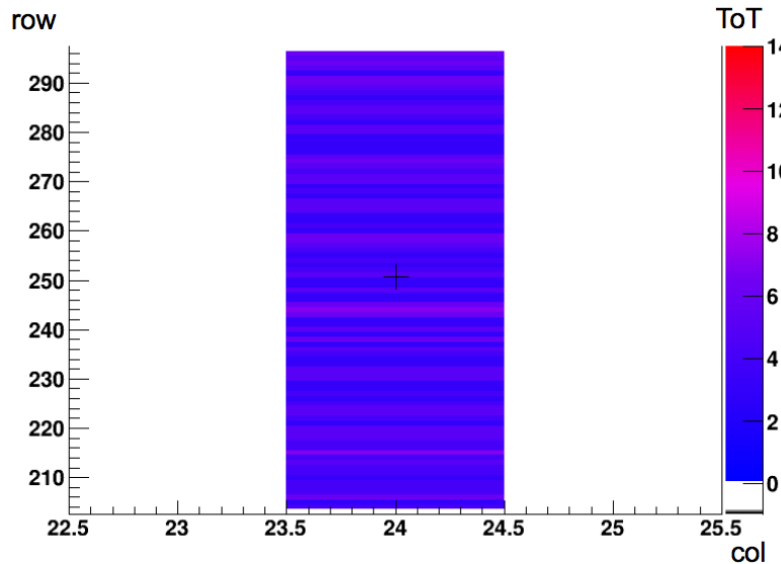
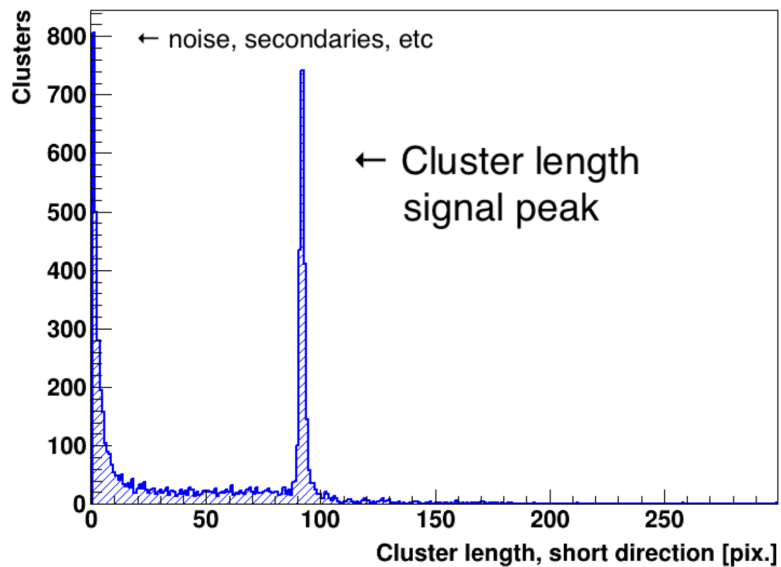


Figure credit:
JUDITH analysis software documentation

Long Pixel Clusters Observed



- Example of typical clusters at $\sim 2.5^\circ$ ($\eta \sim 3.8$)
- Planar module biased at -180V and with 1000e threshold
- Beam is in “short” (50 μm) direction
- “On-peak” cluster size is 93 pixels

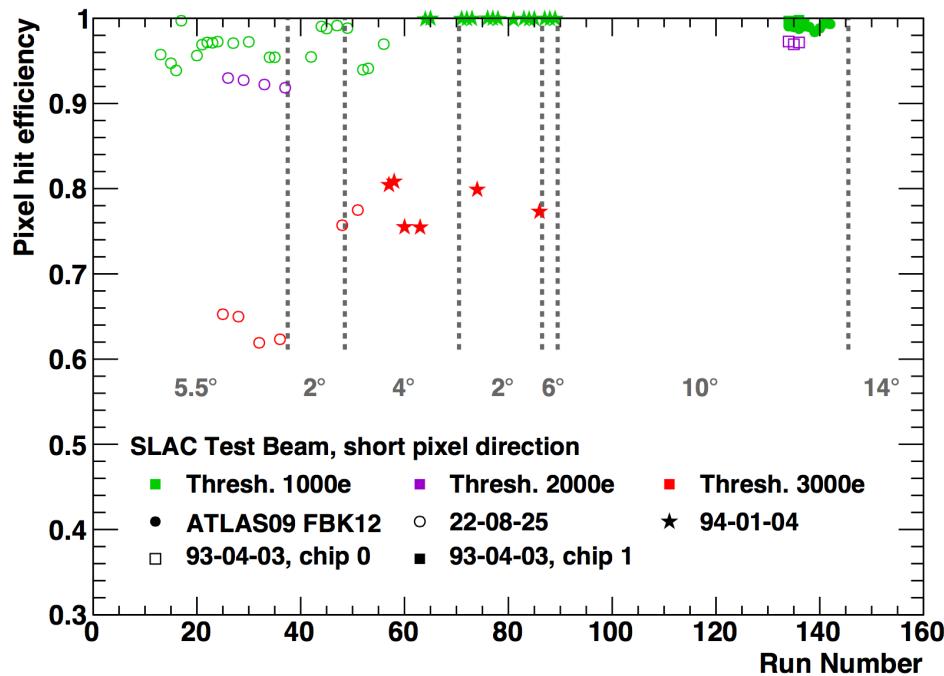


Pixel Hit Efficiency In Test Beam Data

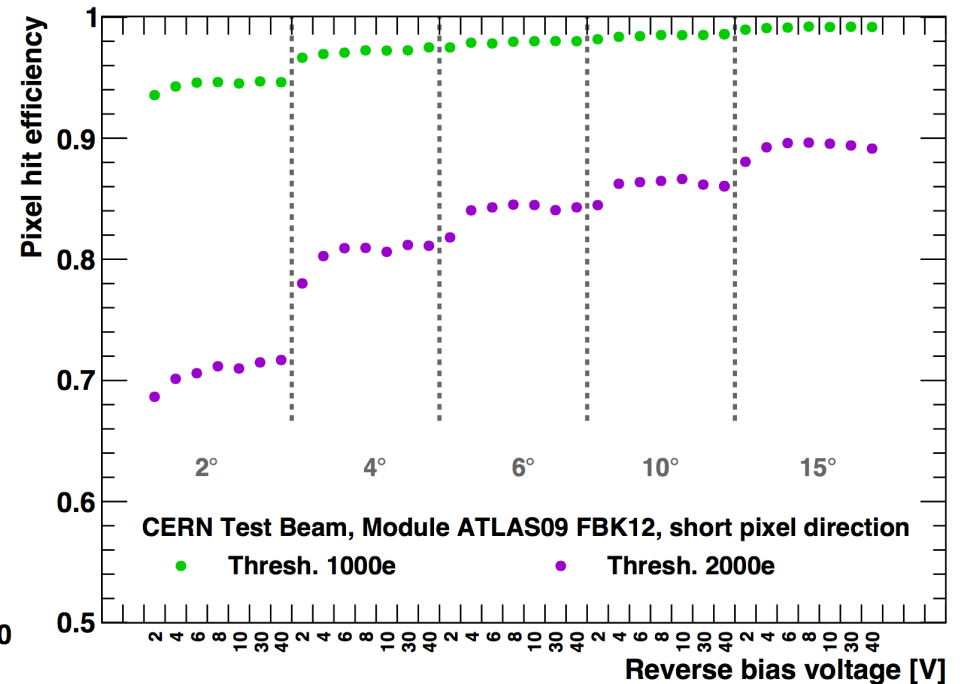
- Efficiency for “long” direction is >99.5% for all modules at all angles, thresholds and reverse bias voltages
- Efficiency for “short” direction has strong dependence on threshold
 - Efficiency in 3D modules also shows some dependence on incidence angle and reverse bias voltage



No timing cut applied



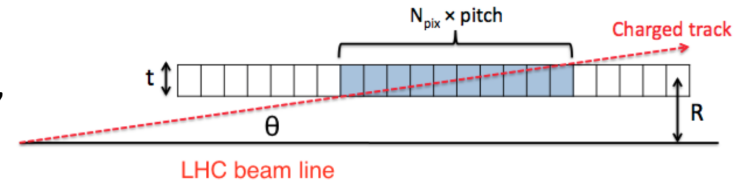
Example: $\epsilon = 4/5$ for this long cluster



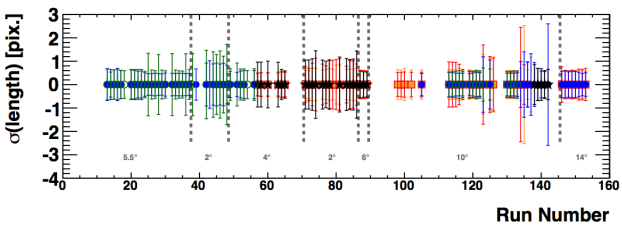
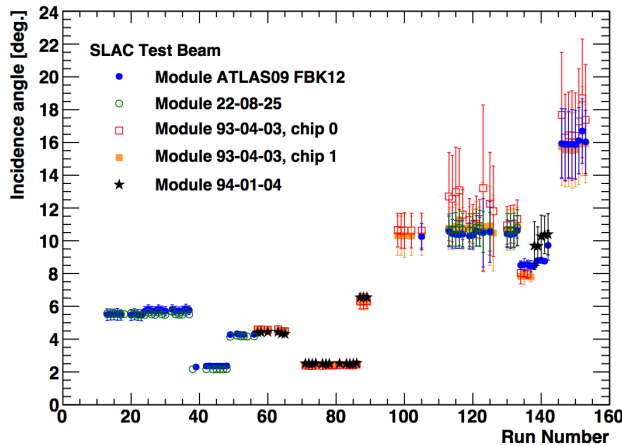
Cluster Length And Measurements Of Incidence Angle

- Cluster length provides precise measurement of incidence angle
 - Results are essentially independent of the threshold
- Consistent results between “short” and “long” directions in SLAC and CERN data
 - ~2% resolution is achieved for $\tan\theta$ at $\theta \sim 2^\circ$ for “short” direction

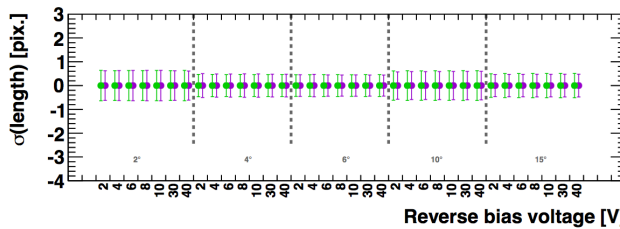
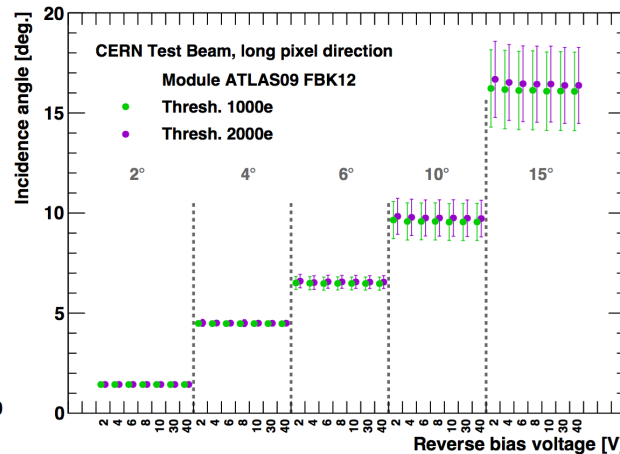
$$\tan\theta = \frac{t}{(N_{pix} - \delta) \times p}, \quad \delta = 1$$



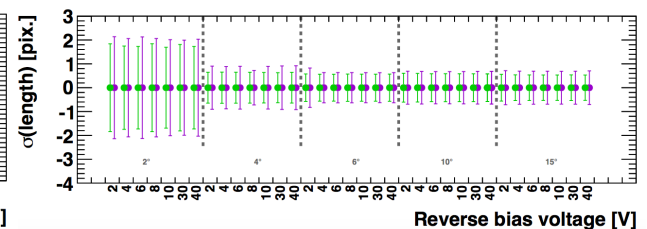
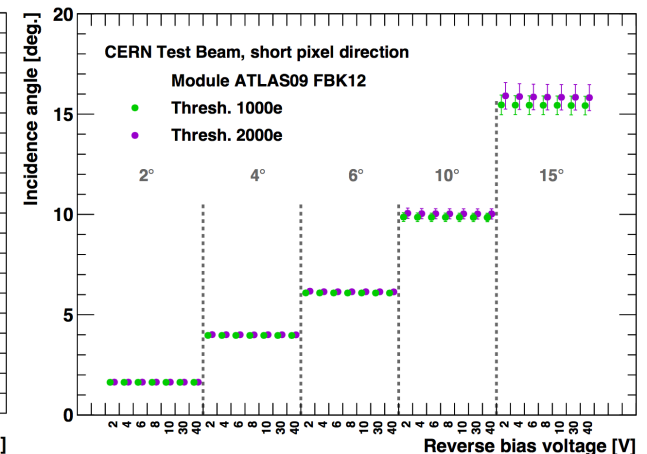
SLAC data



CERN data: 250μm direction

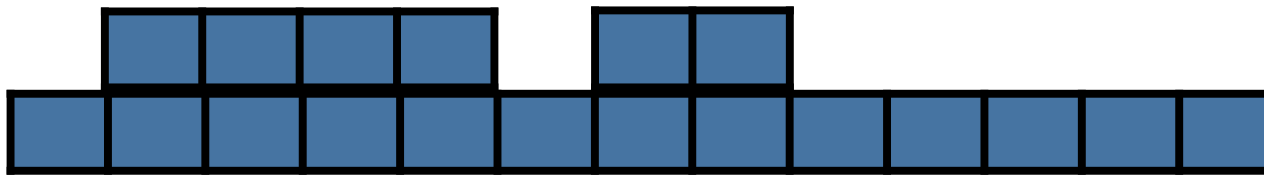


CERN data: 50μm direction



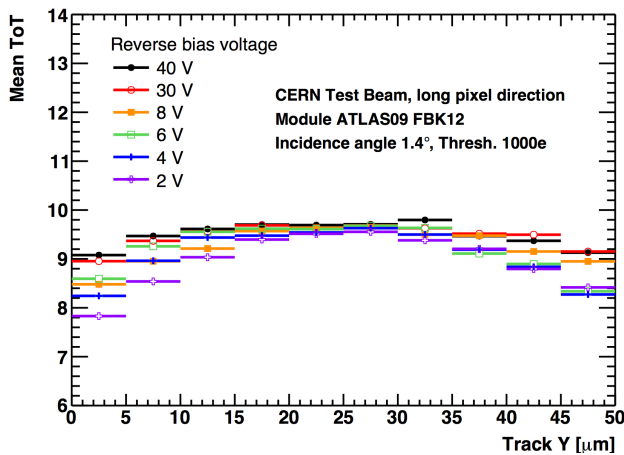
Measurements Of Charge Sharing And Charge Collection

- Measurements performed using CERN data for 3D module as a function of reversed bias voltage
- Charge collection is smaller closer to pixel edges, effect is more pronounced at smaller bias voltages
- Charge sharing is larger at pixel edges and lower bias voltage

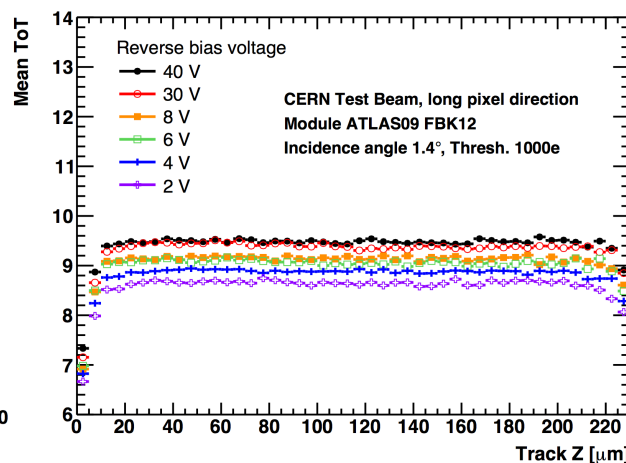


N_m : number of pixels in main row
 N_n : number of pixels in neighboring row

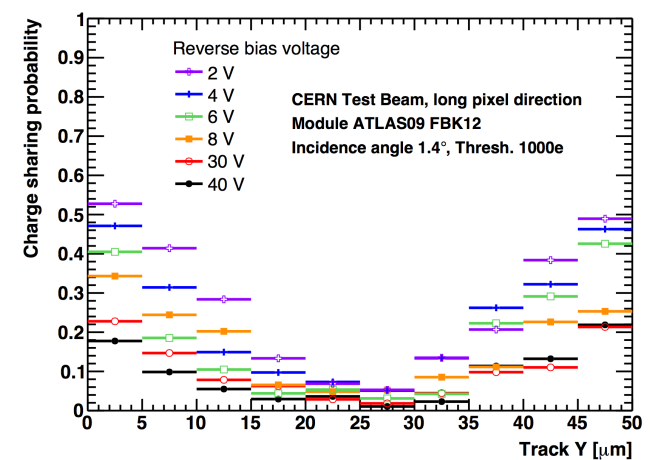
$$P_{sh} = 1 - \frac{N_m - N_n}{N_m + N_n}$$



Direction perpendicular to beam



Sensor depth

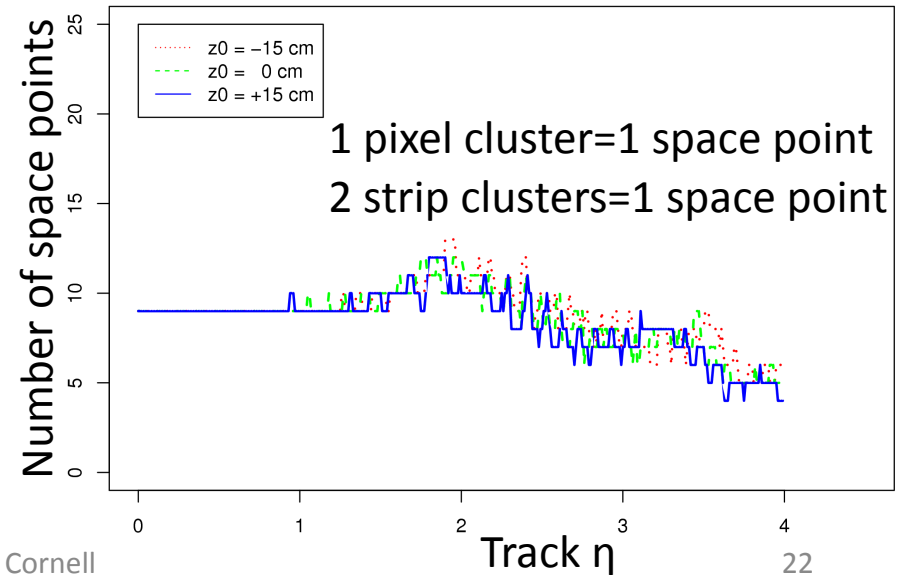
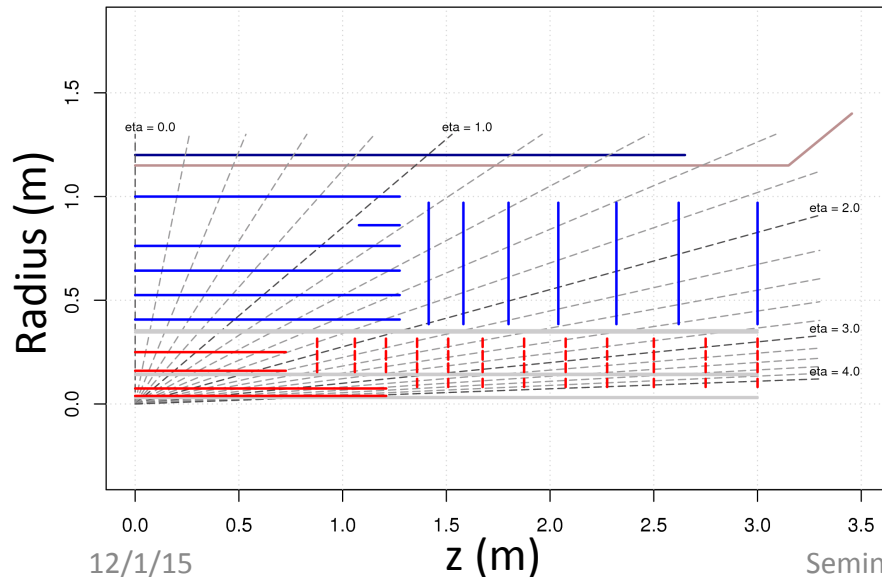


Small Angle Test Beam: Summary

- Long pixel clusters observed: confirmed the concept
- Precise measurement of the incidence angle based on cluster length
 - Essentially the same precision is achieved for 1000e and 2000e thresholds
- Pixel hit efficiency for 50 μ m pitch along the beam direction is >94%
 - Observed dependence on incidence angle
 - Efficiency strongly degrades with increasing threshold
 - As low as 70% efficiency at 2° incidence angle and 2000e threshold
 - Low thresholds are needed to ensure high pixel hit efficiency
- Charge collection and charge sharing show dependence on reverse bias voltage
- Next steps
 - Compare test beam results with simulation
 - Understand dependence of pixel hit efficiency dependence on incidence angle
 - Test beam studies with irradiated modules

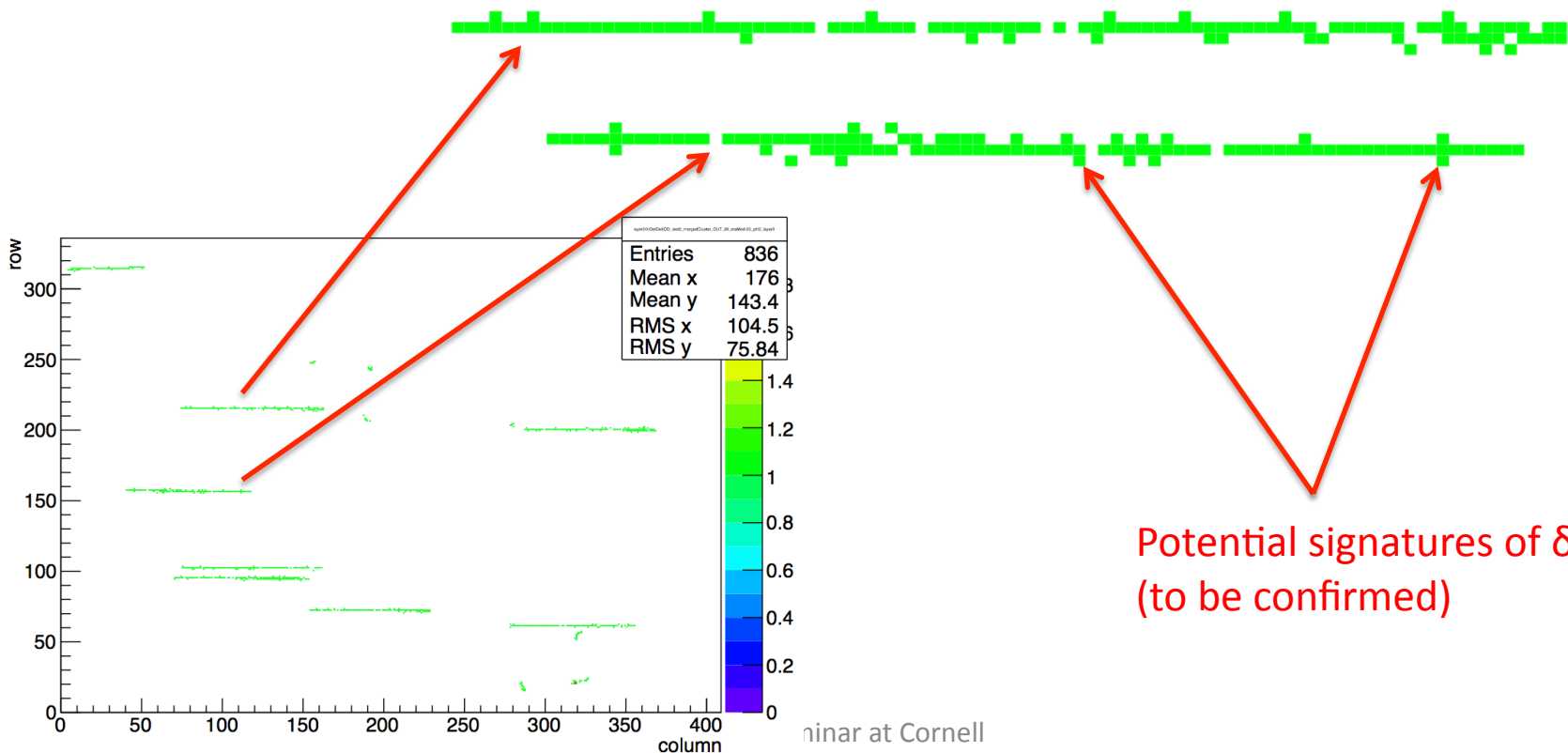
Extended Inner Barrel Layers In Simulation

- Simulated layout is used to prove the concept of forward tracking based on the cluster size, to develop software tools and to gain understanding of potential benefits and issues
 - Pixel detector: 4 barrel layers and up to 12 disks on each side
 - (Inner most) Layer-0 coverage up to $|\eta| < 4$
 - Pixel pitch: $50 \times 50 \times 150 \mu\text{m}^3$ (Width \times Length \times Thickness)
 - Electronics threshold at 700e
 - Ttbar sample without pile-up ($\langle\mu\rangle=0$) and with pile-up ($\langle\mu\rangle=50, 100, 200$)



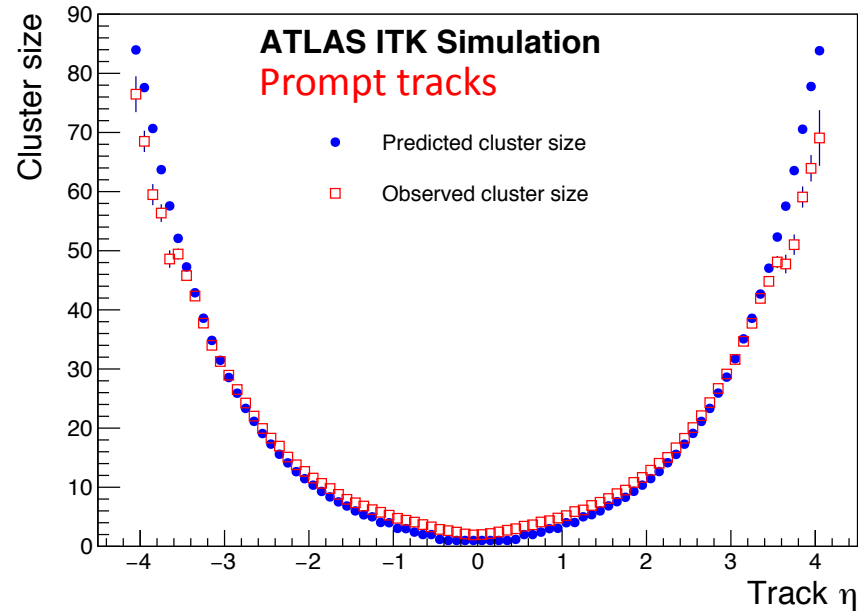
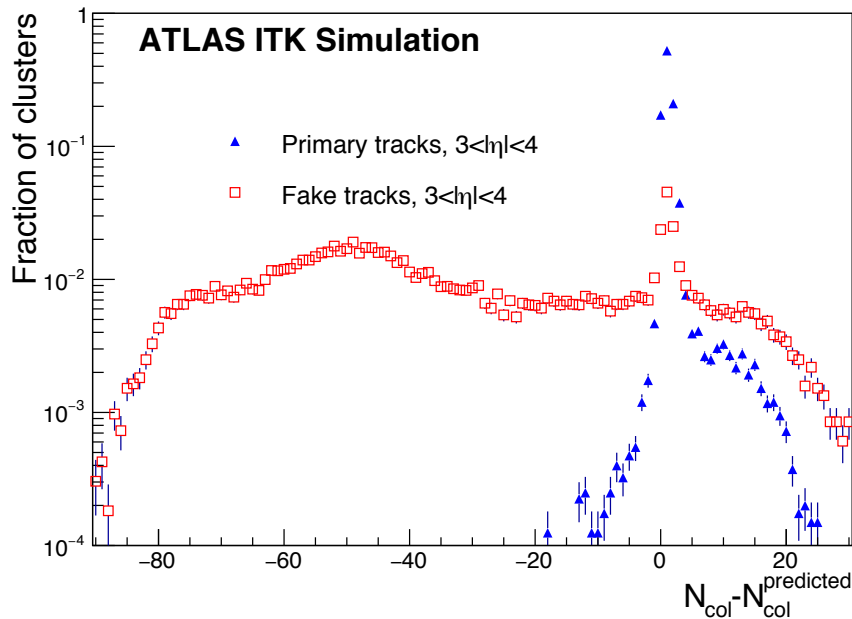
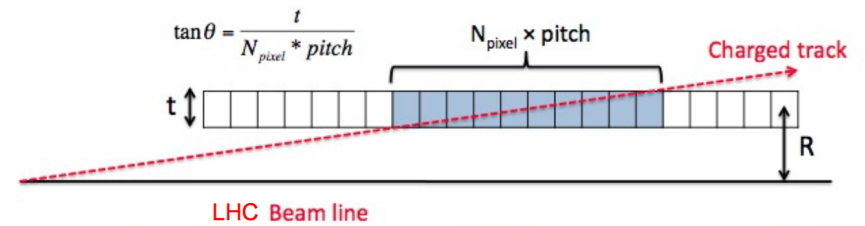
Long Pixel Clusters In Simulation

- Example of typical clusters at $|\eta| \sim 4$
- Almost every long cluster is broken into several fragments
 - Pixel hit efficiency in simulation to be compared with test beam data
 - Unlike test beam, charge is integrated inside 25ns time window
 - Need clustering algorithm to merge broken clusters
- Efficiency for long clusters is essentially 100%



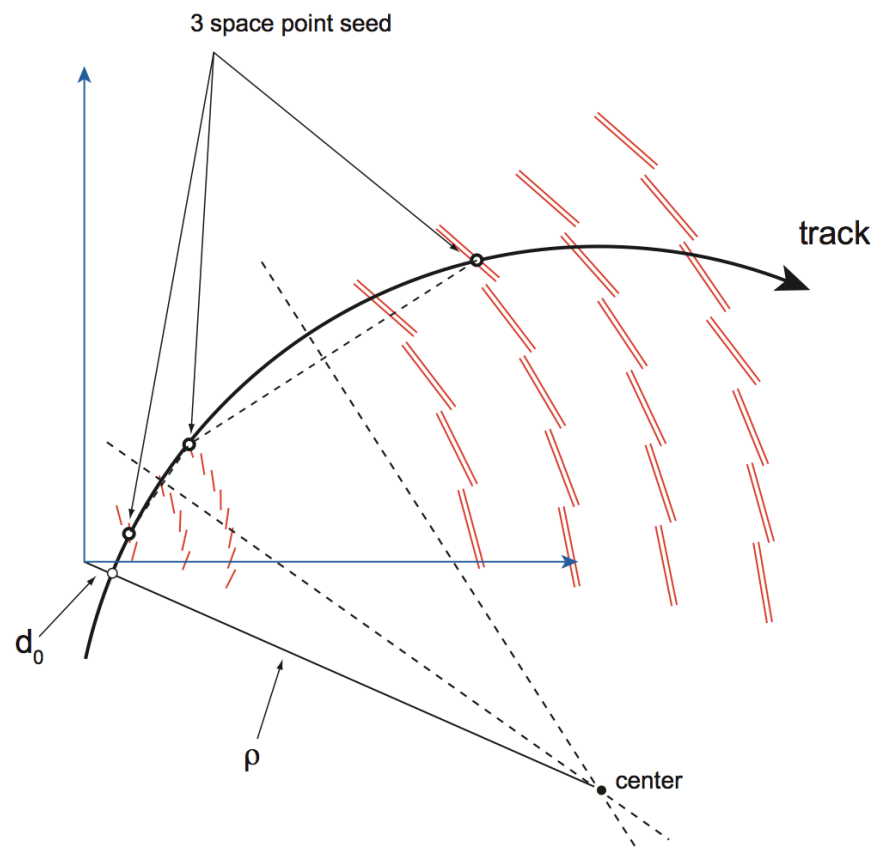
Size Of Pixel Clusters From Prompt And Fake Tracks

- Pixel clusters from prompt tracks follow $N_{col} = \text{thickness} / (\text{pitch} * \tan\theta)$ dependence very well
 - Tracks originating from pile-up and secondary interactions follow the same trend
- Most pixel clusters from fake tracks tend to have clusters size incompatible with $N_{col} = \text{thickness} / (\text{pitch} * \tan\theta)$ dependence
 - Fake tracks are often made of random combination of pixel clusters



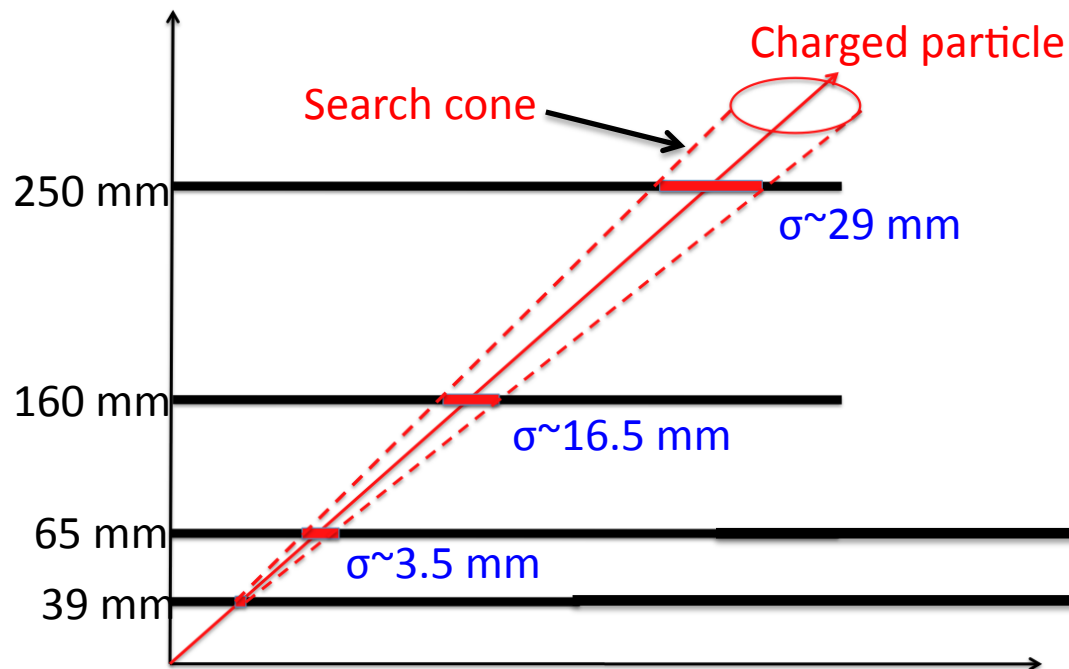
Pattern Recognition At ATLAS

- Track seed= 3 space points
 - Space point provides 3D measurement
 - 1 pixel cluster = 1 space point
 - 2 strip clusters = 1 space point
 - All possible combinations of space points are considered
 - Multiple seeds per track are created
 - Quality cuts applied to reduce number of fake seeds
 - Large number of fake seeds at 200 pile-up interactions
- Seeds provide initial estimates of track parameters
- Search for additional hits along road extrapolated from a seed
- Resolve combinatorial ambiguities due to large number of candidates per track
- Seed creation is most CPU extensive stage of track reconstruction



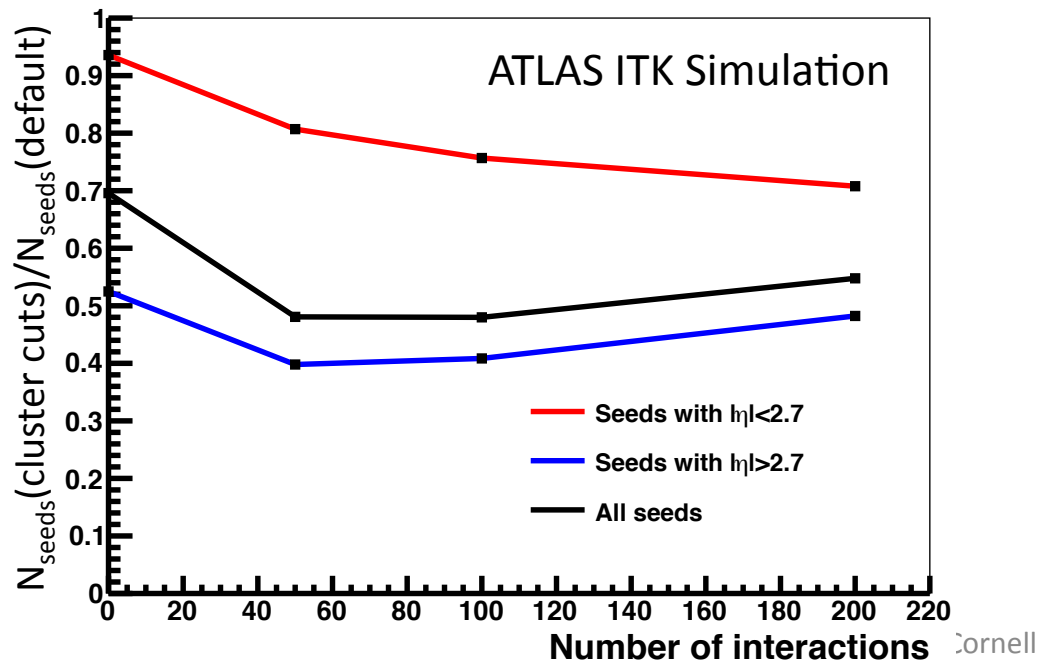
Pattern Recognition Based On Cluster Size: Concept

- **Strategy-1:** reject seeds with pixel clusters whose size is incompatible with θ_{seed}
 - This strategy is currently used in pattern recognition studies
- **Strategy-2:** search for clusters in small cone determined by cluster size in inner layers
 - This strategy potentially offers more advantages (like speed and lower fake rate), but it requires very good understanding and modeling of pixel cluster size
 - To be implemented in the future

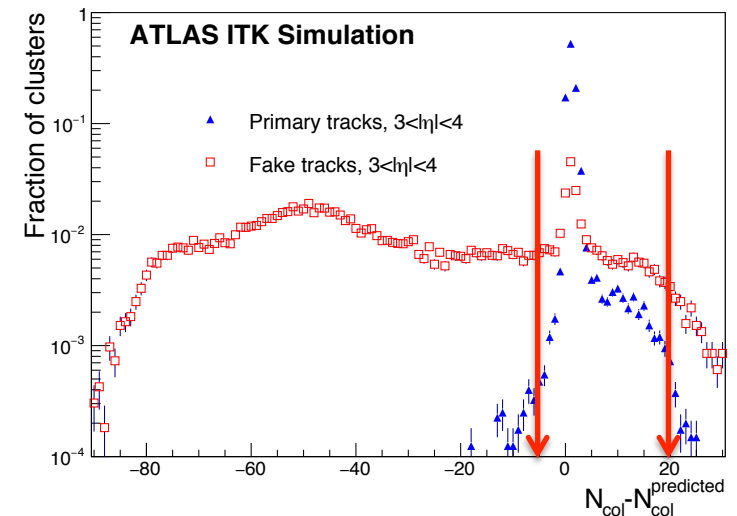


Pattern Recognition Based On Cluster Size: Performance

- About 70% of track seeds in $t\bar{t}$ events with 200 pile-up collisions are in the forward region ($|\eta| > 2.7$)
 - Seed creation is responsible for $\sim 55\%$ of total CPU time per event
- Cluster size information helps to reduce the number of central ($|\eta| < 2.7$) and forward ($|\eta| > 2.7$) seeds by $\sim 30\%$ and $\sim 50\%$, respectively
 - Reduction in the number of seeds will lead to reduction in CPU time per event

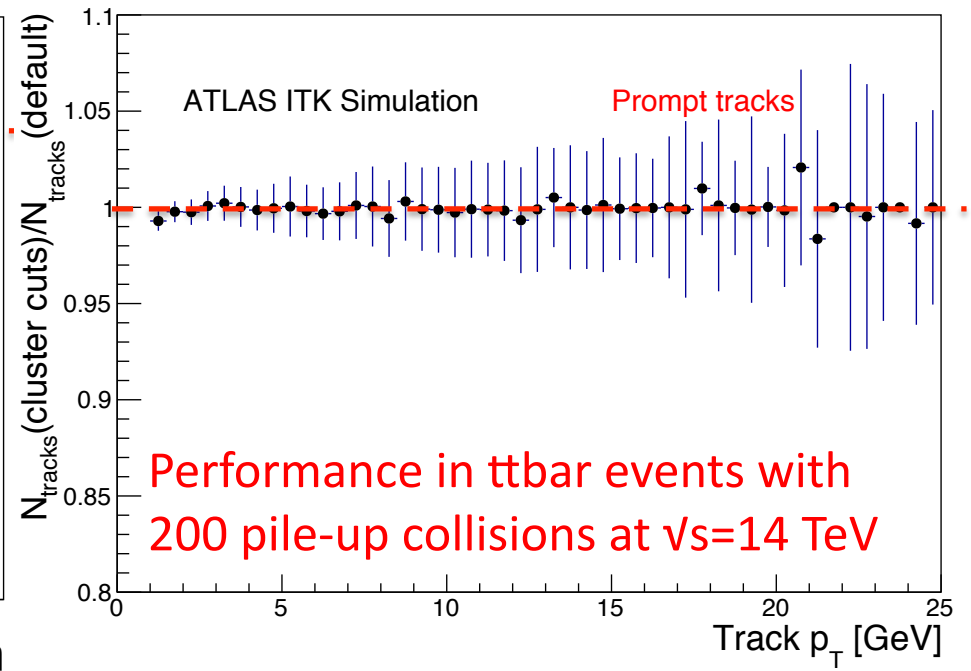
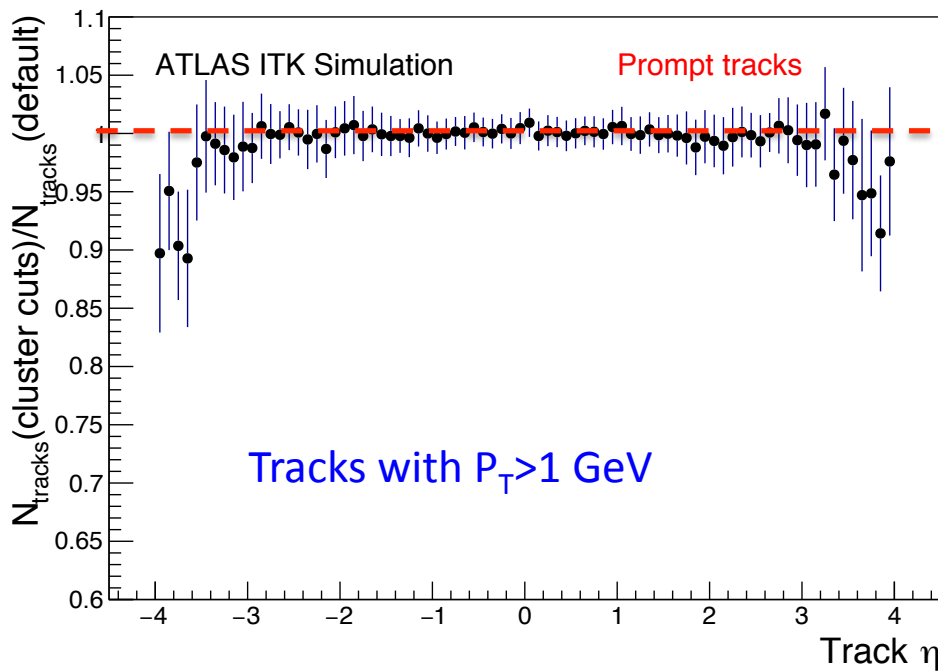


Performance in $t\bar{t}$ events with 200 pile-up collisions at $\sqrt{s}=14$ TeV



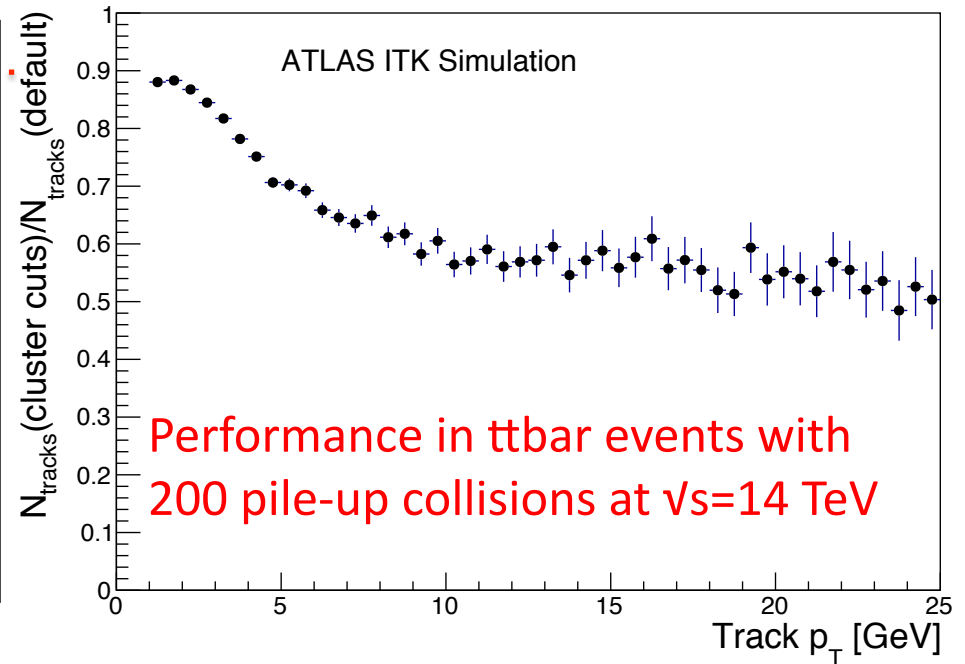
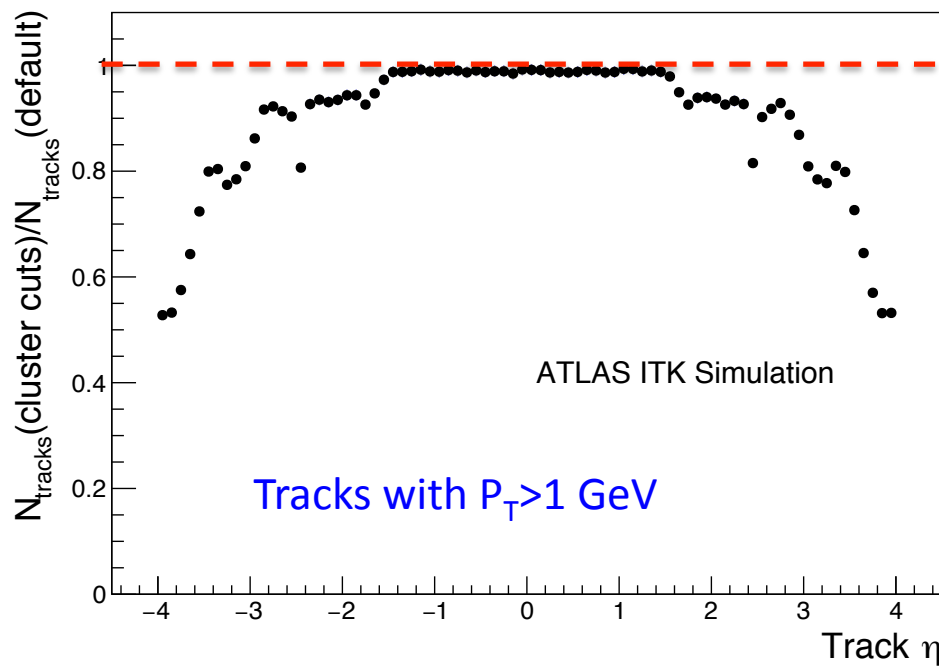
Efficiency For Prompt Tracks

- Large reduction in the number of seeds does not have a significant impact on the number of reconstructed prompt tracks
 - Preliminary results; optimization studies are still in progress
 - $N_{\text{tracks}}(\text{new})$: number of tracks reconstructed with pattern recognition exploiting cluster size information
 - $N_{\text{tracks}}(\text{default})$: number of tracks reconstructed with default pattern recognition



Reduction In The Number Of Fake Tracks

- **Default pattern recognition:** most of the reconstructed tracks in the very forward region ($|\eta| > 3.5$) are fakes
- **New pattern recognition:** large reduction in the number of fake tracks in the forward region with minimal impact on tracks from hard scattering and pile-up interactions
 - Preliminary results; optimization studies are still in progress



Pattern Recognition With Long Clusters: Summary

- Long clusters can be used to improve pattern recognition
- Cluster size in simulation follows predicted pattern
 - Cluster segments can be efficiently merged to restore the original cluster
- Large difference between size of clusters attached to prompt and fake tracks
- Use of cluster size information in pattern recognition allows for significant reduction in the number of seeds and will potentially lead to significant reduction in CPU time
- Reduction in the number of seeds is achieved at a minimal impact on the reconstruction efficiency for prompt tracks
- Use of cluster size information in pattern recognition allows for significant reduction in the number of fake tracks

Conclusions

- ATLAS R&D program for Phase-2 all-silicon tracker upgrade is well underway
 - Strip TDR is due in 2016
 - Pixel TDR is due in 2017
- Extensive studies are in progress for the layout of the tracking detector with coverage up to $|\eta| < 4$
- Two competing concepts for the Pixel detector layout
 - “Extended” barrel layers
 - “Inclined” barrel modules
- “Extended” barrel layout utilizes cluster size information for improvements in pattern recognition
 - Concept is proven in test beam studies
 - Simulation studies indicate significant benefits for track reconstruction

Backup

End-Cap Pixel Detector

28-quad ring shown

- active radial coverage 95mm-135mm
- Modules closer together on this ring than in the outer layers
- **Not part of current Unity layouts** but illustrates the concept...

